Supporting Information for "Distribution of interseismic coupling along the North and East Anatolian Faults inferred from InSAR and GPS data"

Quentin Bletery[1], Olivier Cavalié[1], Jean-Mathieu Nocquet[1,2] and Théa Ragon[3]

[1]Université Côte d'Azur, IRD, CNRS, Observatoire de la Côte d'Azur, Géoazur, France

[2]Institut de Physique du Globe de Paris, Université de Paris, CNRS, France

[3]Seismological Laboratory, California Institute of Technology, USA

Contents of this file

March 2, 2020, 4:05pm

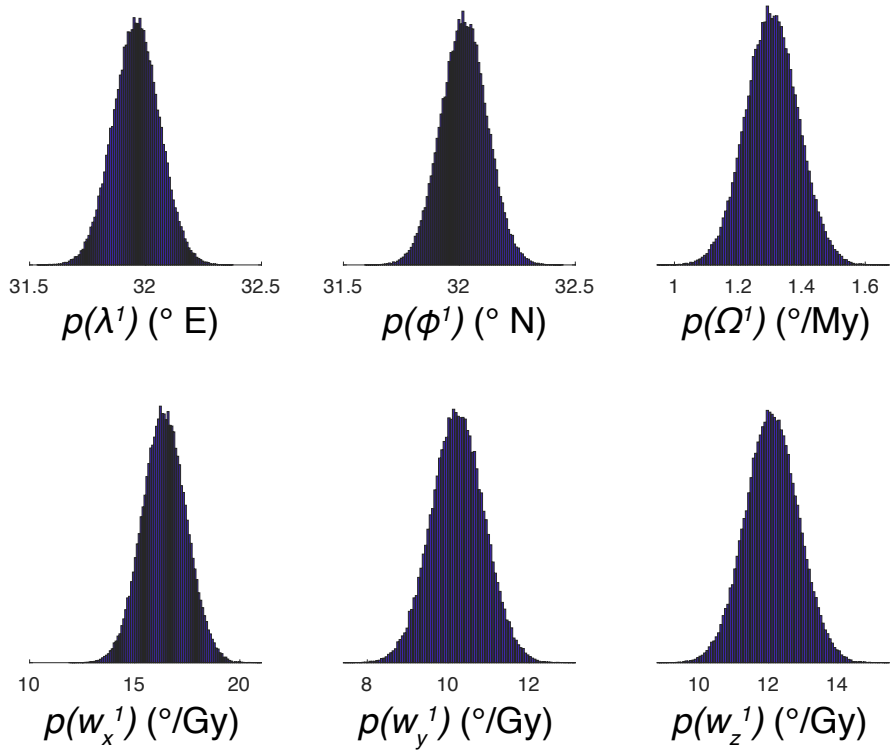

Figure S1. Top: prior pdfs of the Euler pole coordinates $p(\lambda^1)$, $p(\phi^1)$ and angular velocity $p(\Omega^1)$ of the Anatolian plate with respect to Eurasia. Bottom: corresponding prior pdfs of the rotation vector in Cartesian geocentric coordinates (in 10^{-9} °/y).

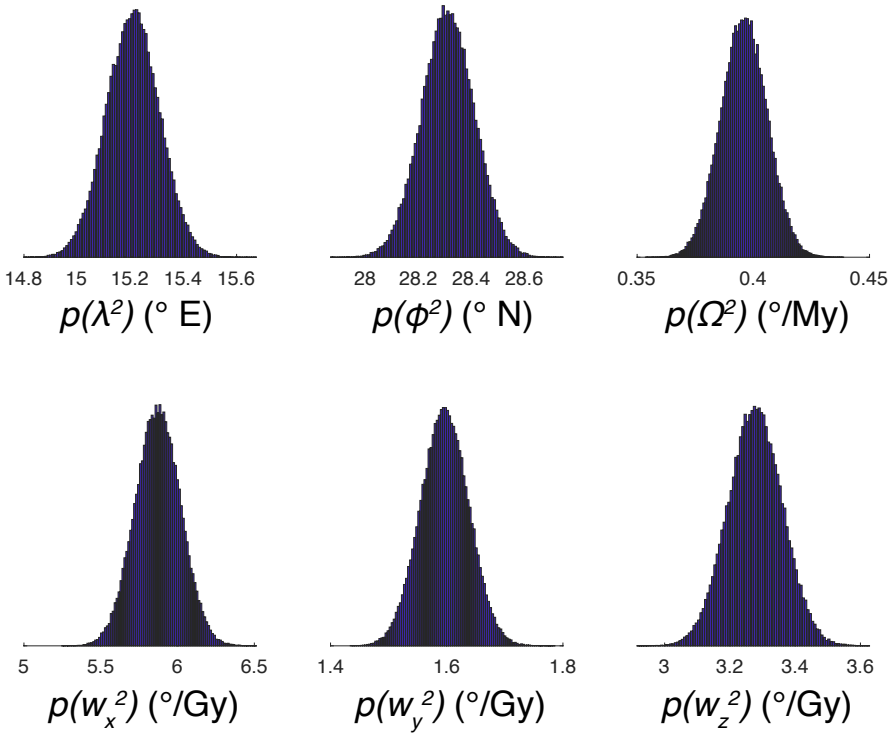

Figure S2. Top: prior pdfs of the Euler pole coordinates $p(\lambda^2)$, $p(\phi^2)$ and angular velocity $p(\Omega^2)$ of the Arabian plate with respect to Eurasia. Bottom: corresponding prior pdfs of the rotation vector in Cartesian geocentric coordinates (in 10^{-9} °/y).

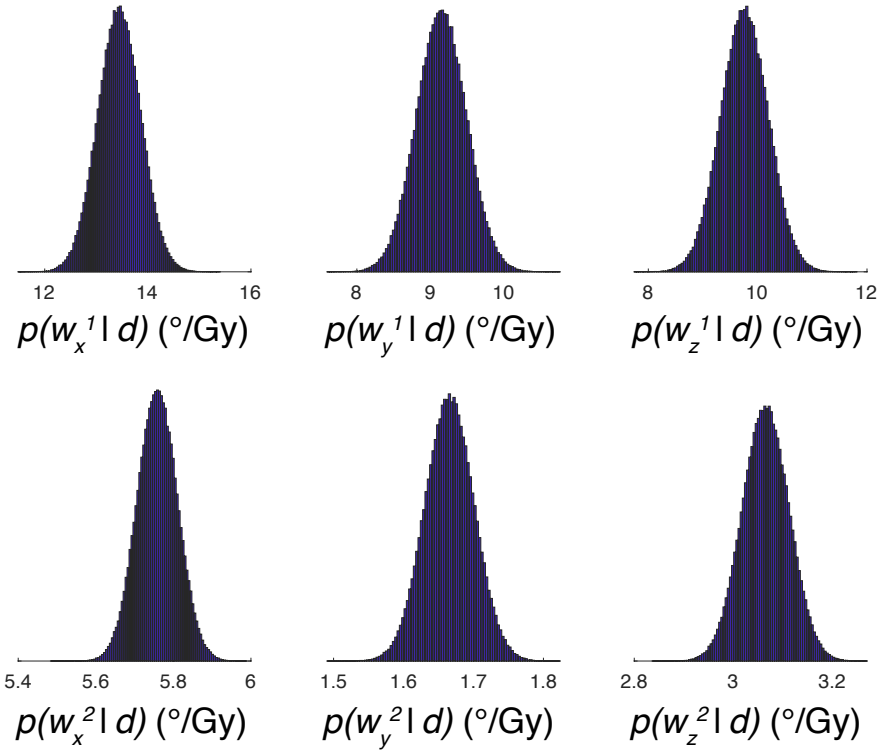

Figure S3. Posterior pdfs of the rotation vectors $\mathbf{w^1}$, $\mathbf{w^2}$ in Cartesian geocentric coordinates (in 10^{-9} °/y).

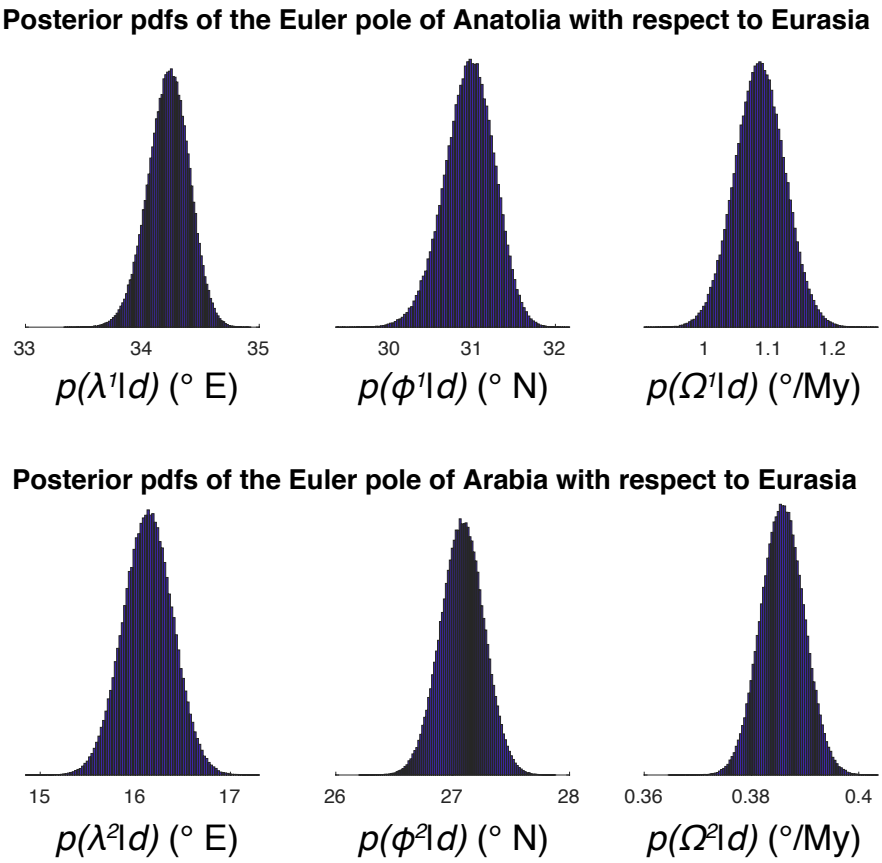

Figure S4. Posterior pdfs of the Anatolian and Arabian Euler pole coordinates and angular velocities with respect to Eurasia.

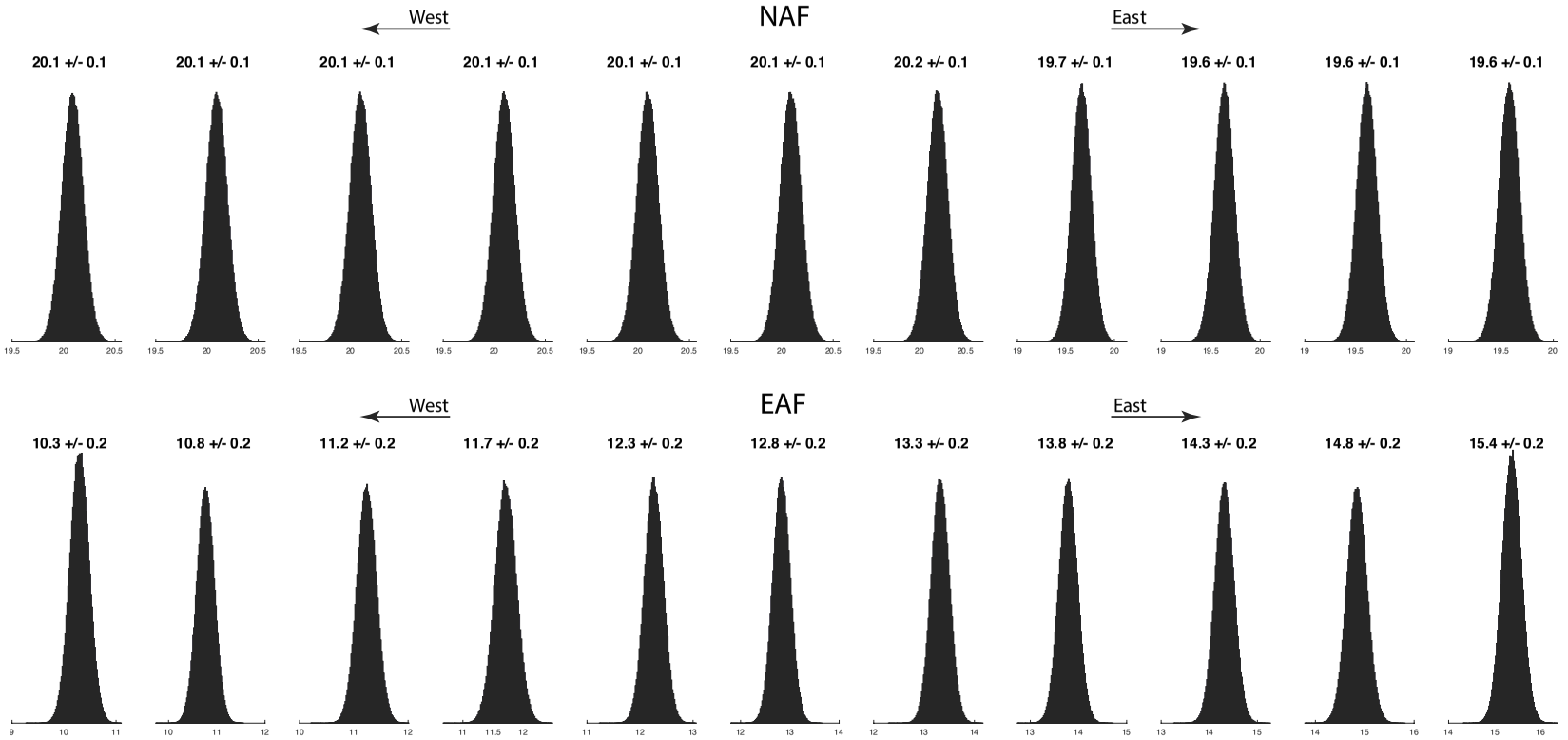

Figure S5. Posterior pdfs of long term plate motion rate projected along both faults. Positions correspond to positions of the deepest patches along the faults in Fig. 2. Values at the top of each pdf indicate the pdf mean and standard deviation (in mm/year).

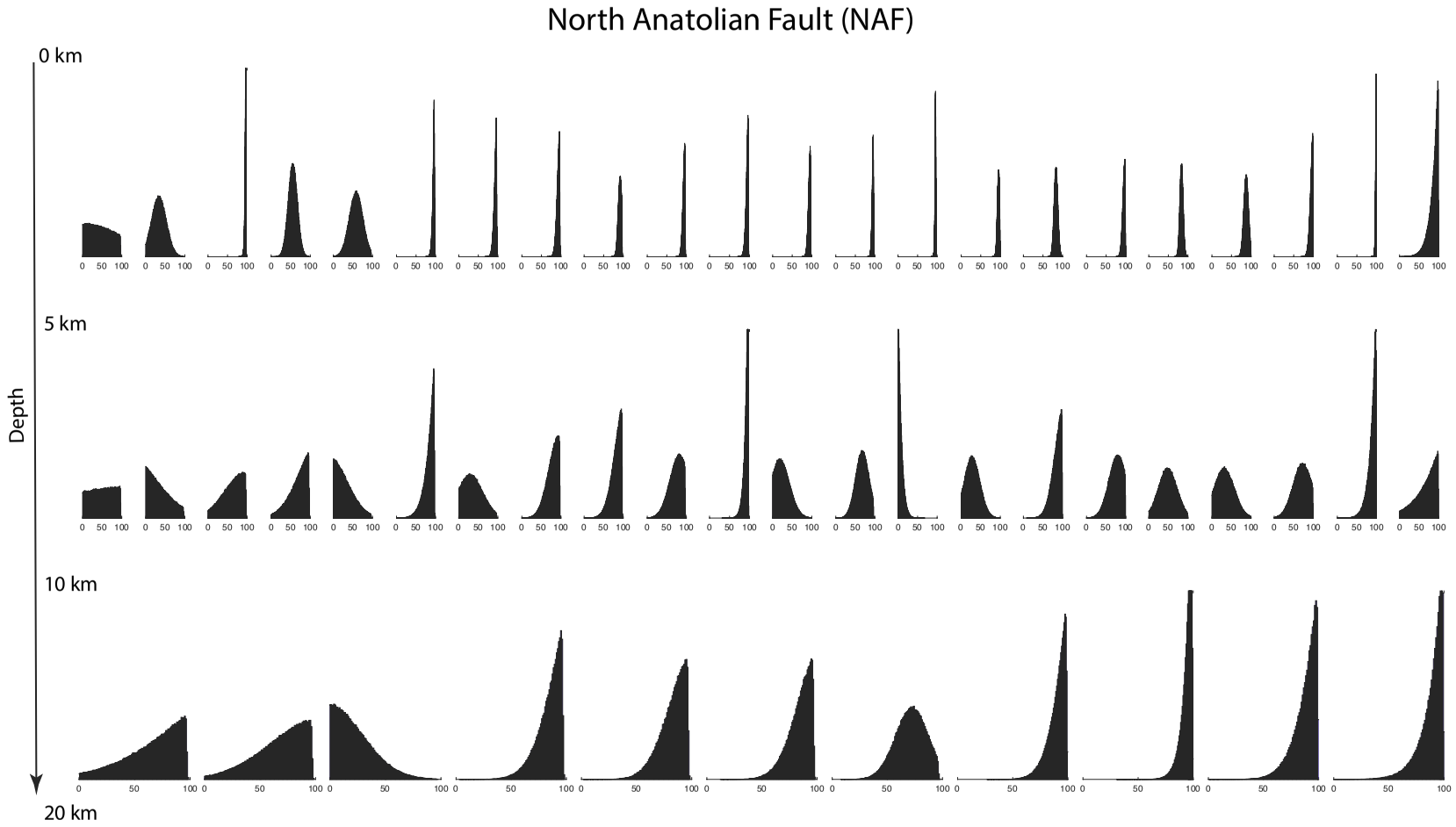

Figure S6. Posterior pdfs of each coupling coefficient along the NAF. Positions correspond to positions along the faults in Fig. 2.

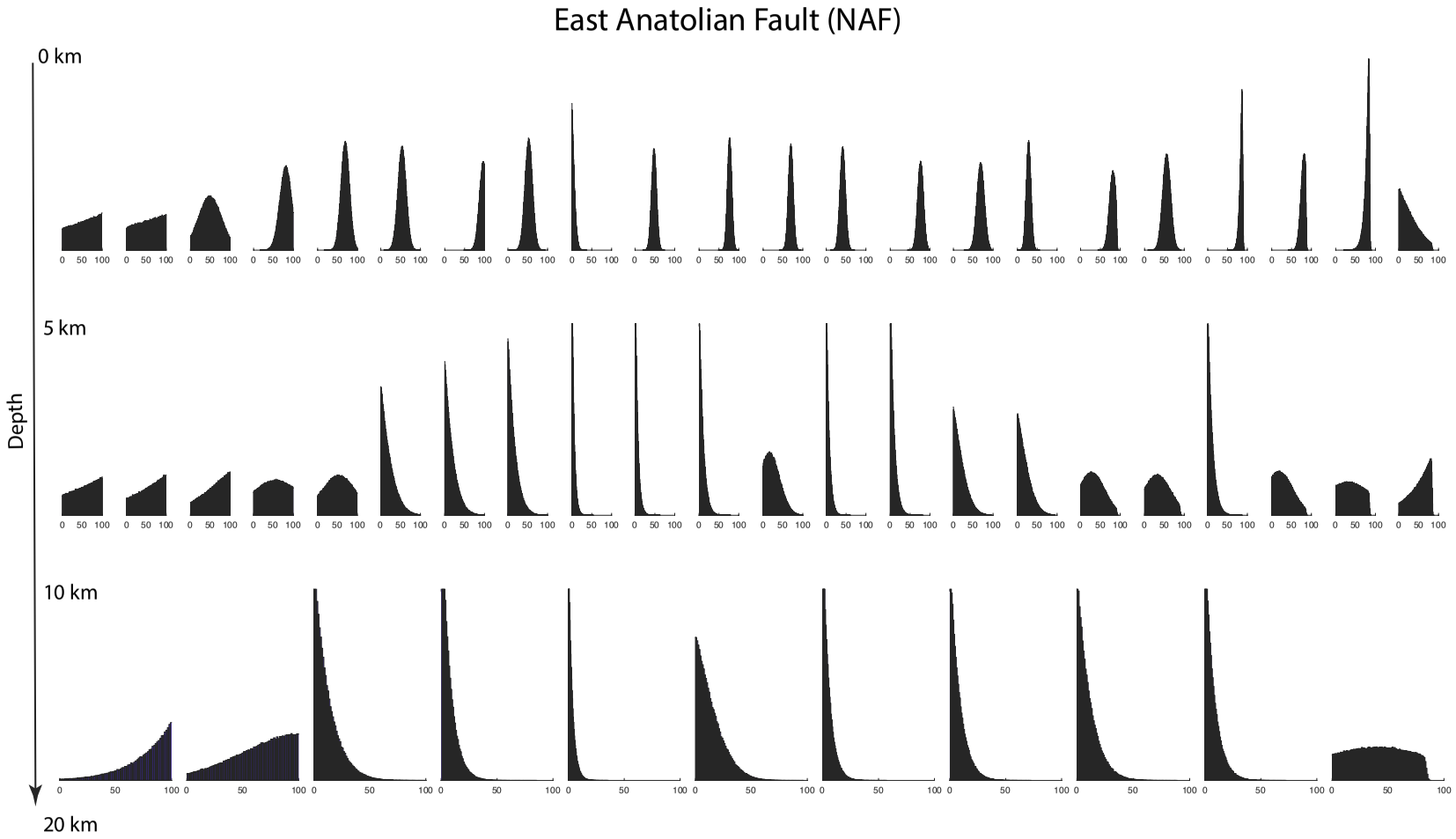

Figure S7. Posterior pdfs of each coupling coefficient along the EAF. Positions correspond to positions along the faults in Fig. 2.

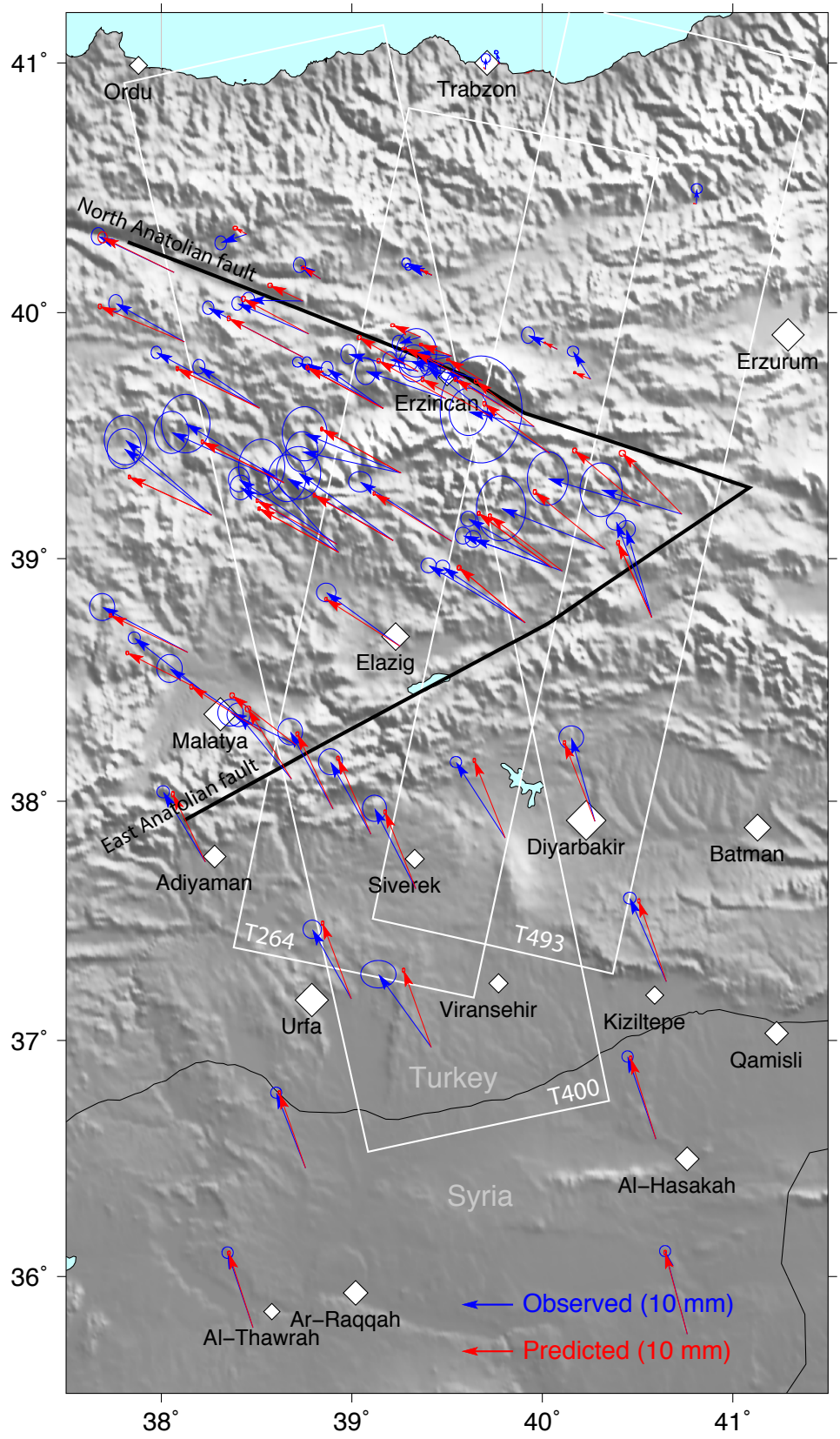

Figure S8. Observed (blue) and predicted (red) GPS measurements with their 2-σ ellipses of uncertainties. Black lines show the fault traces. White contours show contours of InSAR tracks used in the inversion.

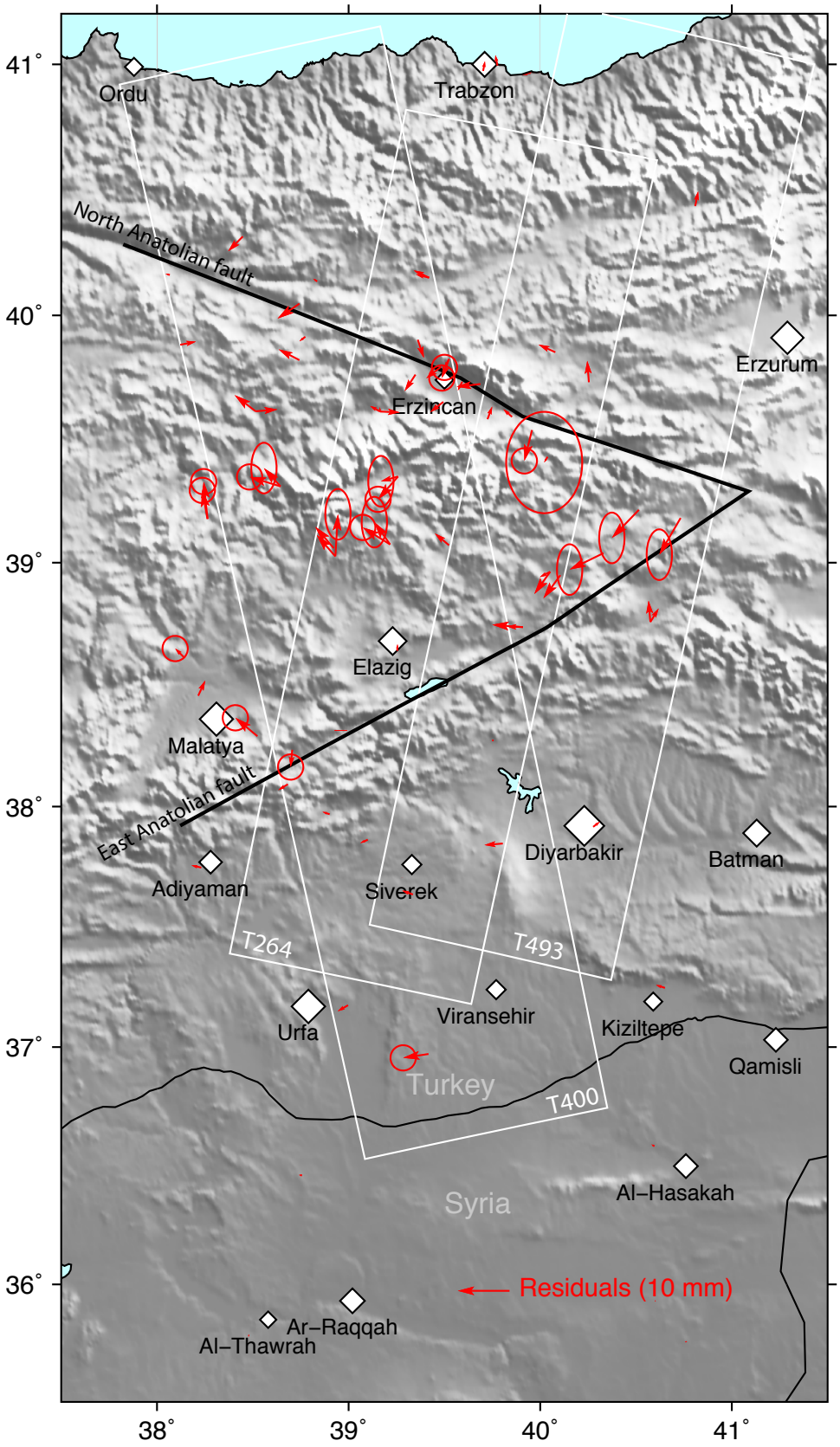

Figure S9. GPS Residuals. Ellipses are summed 2-σ standard deviations of the observed and predicted data.

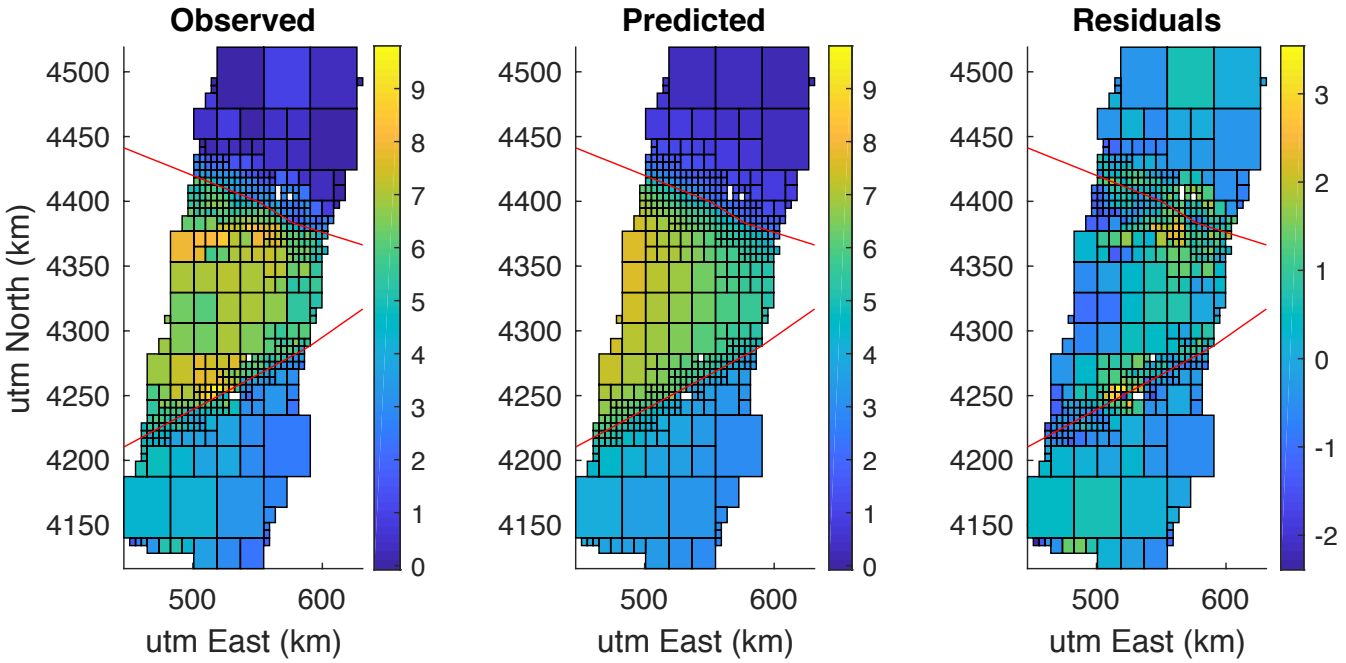

Figure S10. Observed (left), predicted (center), and residual (right) sub-sampled SAR interferograms for Track T264. Red lines indicate the fault traces.

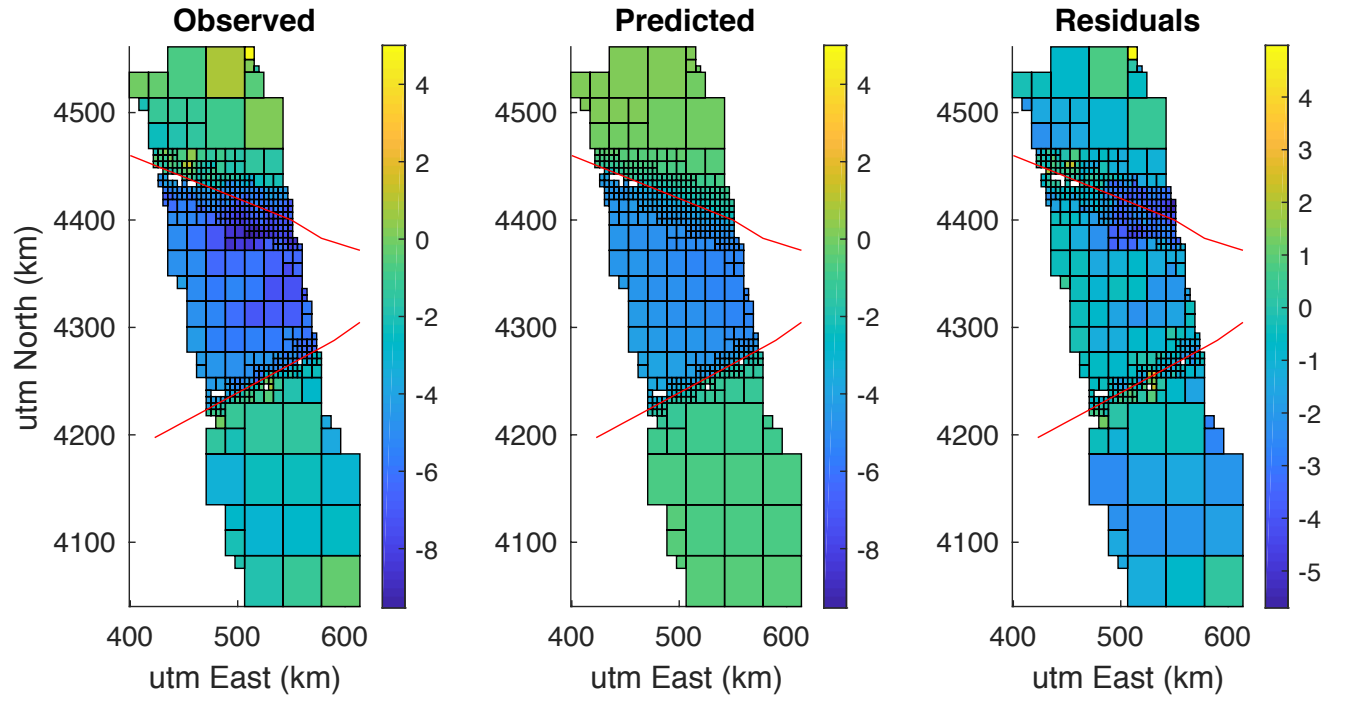

Figure S11. Same as Fig. S10 for track T400.

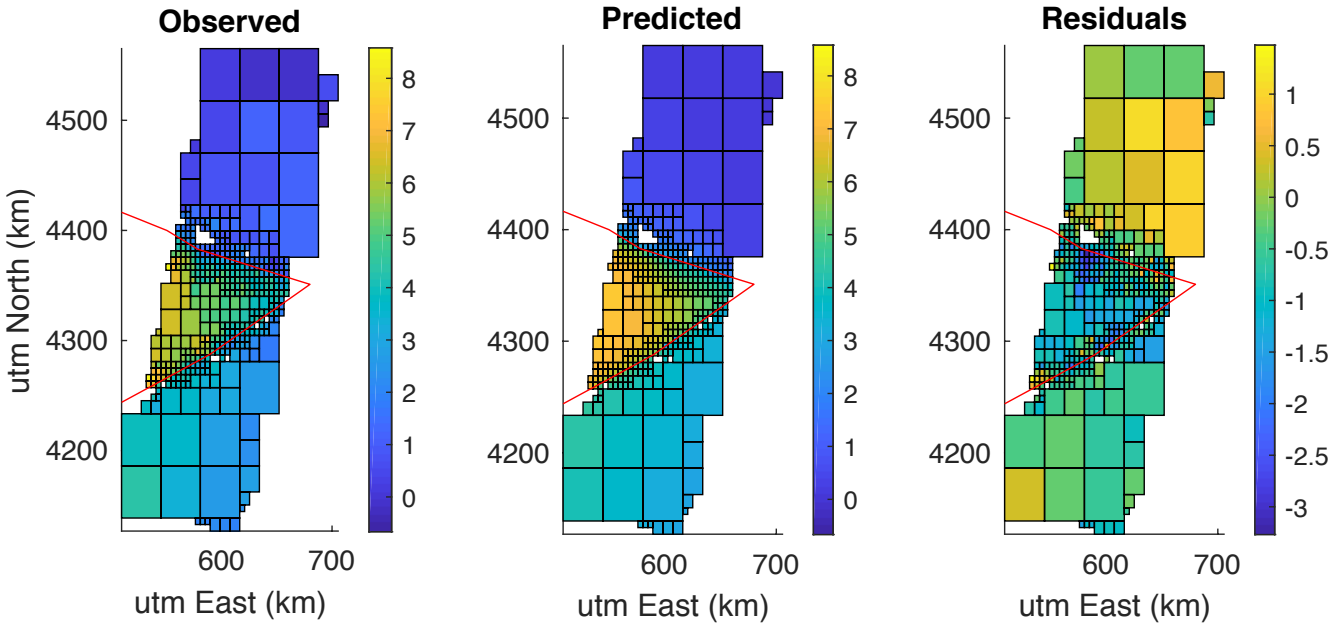

Figure S12. Same as Fig. S10 for track T493.

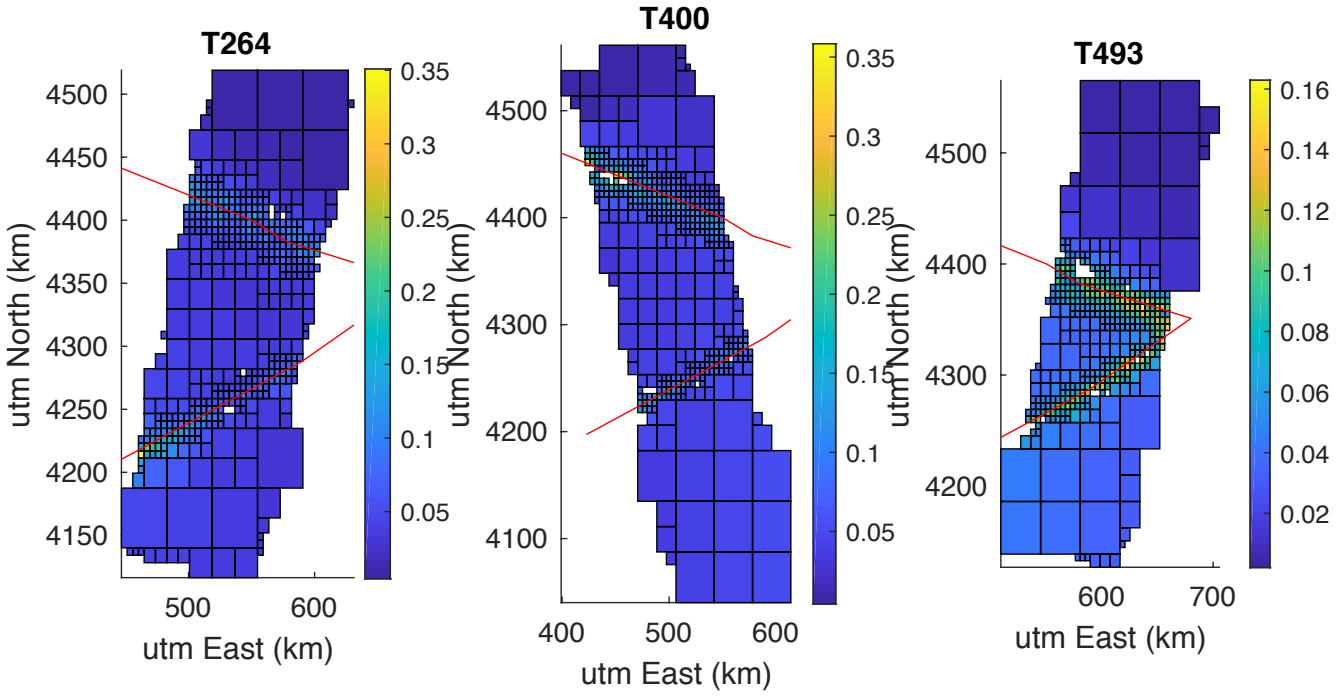

Figure S13. Standard deviation of the predicted interferograms.